

See discussions, stats, and author profiles for this publication at: <https://www.researchgate.net/publication/231703526>

# Three-Dimensional Crystalline Structure of Cellulose Triacetate II

ARTICLE *in* MACROMOLECULES · JANUARY 1978

Impact Factor: 5.8 · DOI: 10.1021/ma60061a016

---

CITATIONS

62

---

READS

17

## 5 AUTHORS, INCLUDING:



Pudupadi R Sundararajan

Carleton University

127 PUBLICATIONS 2,237 CITATIONS

[SEE PROFILE](#)

at the tip of the cell. At this point ESR signal intensity measurements were made against a Mn<sup>2+</sup> marker every 15 min. Measurements involved bringing the cell tip rapidly to room temperature with a 5-s immersion in water and scanning the signal and marker. The measurement time was 4 min and is not included in the polymerization time.

In the case of the additive nitric oxide, a second signal in the ESR spectrum, having a central line at a lower magnetic field and wing structure between 20 and 30 G on either side, overlapped the normally observed 2.3 G signal (Figure 14). The spectrum did not change as polymerization proceeded. Evacuation of the cell for 1 h did not change the spectrum indicating it is not a weak association of polymer with the nitric oxide molecule. When preformed polymer was exposed to nitric oxide, a shoulder maximum on the ESR signal slowly developed at a point corresponding to the new line's central maximum. The nature of the interaction between polymer and nitric oxide is not known.

**Acknowledgment.** The authors are indebted to the Faculty Research Award Program, the City University of New York, Grant No. 1620, 11084, and 11420 and to the donors of the Petroleum Research Fund, administered by the American Chemical Society, for a grant to N.L.Y.

#### References and Notes

- (1) Based in part on a doctoral dissertation submitted by A. W. Snow in partial fulfillment of the requirements for the degree of Doctor of Philosophy at the Graduate School of the City University of New York.
- (2) O. Diels and B. Wolf, *Ber.*, **39**, 689 (1906).
- (3) R. N. Smith, D. A. Young, E. N. Smith, and C. C. Carter, *Inorg. Chem.*, **2**, 829 (1963).
- (4) A. R. Blake, W. T. Eeles, and P. P. Jennings, *Trans. Faraday Soc.*, **60**, 691 (1964).
- (5) (a) E. Ziegler, H. Junek, and H. Bieman, *Monatsh. Chem.*, **92**, 927 (1961); (b) H. Sterk, P. Tritthart, and E. Ziegler, *ibid.*, **101**, 1851 (1970).
- (6) A. Snow, N.-L. Yang, and H. Haubenstock, *Carbon*, **14**, 177 (1976).
- (7) N.-L. Yang, A. Snow, H. Haubenstock, and F. Bramwell, *J. Polym. Sci.*, in press.
- (8) R. N. Smith, *Trans. Faraday Soc.*, **62**, 1881 (1966).
- (9) A. R. Blake, *J. Chem. Soc.*, 3866 (1965).
- (10) C. Walling, "Free Radicals in Solution", Wiley, New York, N.Y., 1957, p 169; I. M. Kolthoff and F. A. Bovey, *Chem. Rev.*, **42**, 491 (1948).
- (11) B. Vollmert, "Polymer Chemistry", Springer-Verlag, New York, N.Y., 1973, p 61.
- (12) T. Kunitake and S. Murakami, *J. Polym. Sci.*, **12**, 67 (1974); E. G. Janzen, *Acc. Chem. Res.*, **4**, 31 (1971).
- (13) R. N. Lacey, "The Chemistry of Alkenes", S. Patai, Ed., Chapter 14, Interscience, New York, N.Y., 1964, Chapter 14.
- (14) G. Hegar, "Beitrag zur Chemie des Kohlensuboxides", Ph.D. Thesis, Zurich, 1961.
- (15) J. March, "Advanced Organic Chemistry: Reactions, Mechanisms and Structure", McGraw-Hill, New York, N.Y., 1968, pp 477 and 478.
- (16) V. L. Schmidt, H. P. Boehm, and U. Hofmann, *Z. Anorg. Allg. Chem.*, **282**, 16 (1955).
- (17) A. R. Blake and A. F. Hyde, *Trans. Faraday Soc.*, **60**, 1775 (1964).
- (18) T. Kappe and E. Ziegler, *Angew. Chem., Int. Ed. Engl.*, **13**, 491 (1974).
- (19) H. Ulrich, "Cycloaddition Reactions of Heterocumulenes", Academic Press, New York, N.Y., 1967, Chapter 3.
- (20) W. H. Smith and G. E. Leroi, *J. Chem. Phys.*, **45**, 1767 (1966).
- (21) E. A. Williams, J. D. Cargiola, and A. Ewo, *Chem. Commun.*, 366 (1975).
- (22) J. F. Olsen and L. Burnelle, *J. Phys. Chem.*, **73**, 2298 (1967); J. R. Sabin and H. Kim, *J. Chem. Phys.*, **56**, 2195 (1972).
- (23) W. Ried and H. Mengler, *Justus Liebigs Ann. Chem.*, **678**, 113 (1964).
- (24) W. J. Baron, M. R. DeCamp, M. E. Hendrick, M. Jones, Jr., R. H. Levin, and M. B. Sohn in "Carbenes", Vol. 1, M. Jones, Jr., and R. A. Moss, Eds., Wiley, New York, N.Y., 1973, p 107.
- (25) P. P. Gaspar and G. S. Hammond, ref 24, Vol. II, 1975, p 319 ff.
- (26) M. Tanaka, T. Nagai, and N. Tokura, *J. Org. Chem.*, **38**, 1602 (1973).
- (27) D. R. Kearns and M. Calvin, *J. Am. Chem. Soc.*, **83**, 2110 (1961).
- (28) C. L. Anygal, G. A. Barclay, A. A. Hurkins, and R. J. W. LeFevre, *J. Chem. Soc.*, 2583 (1951); K. Ingold, *Chem. Rev.*, **15**, 552 (1947).
- (29) D. Bijl, H. Kainer, and A. C. Rose-Innes, *J. Chem. Phys.*, **35**, 765 (1959); J. W. Eastman, G. M. Andrees, and M. Calvin, *ibid.*, **36**, 1197 (1962); L. S. Singer and J. Kommandeur, *J. Phys. Chem.*, **34**, 133 (1961).
- (30) G. Brauer, "Handbook of Preparative Inorganic Chemistry", 2nd ed., Academic Press, New York, N.Y., p 648.
- (31) L. B. Dashkevich and V. G. Berlin, *Russ. Chem. Rev.*, **36**, 391 (1967).
- (32) G. S. Ross and A. R. Glassgow, *Anal. Chem.*, **36**, 700 (1964).

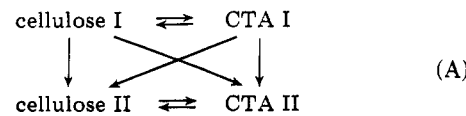
## Three-Dimensional Crystalline Structure of Cellulose Triacetate II<sup>1a</sup>

E. Roche,<sup>\*1b</sup> H. Chanzy,<sup>\*1b</sup> M. Boudeulle,<sup>1c</sup> R. H. Marchessault,<sup>1d</sup> and P. Sundararajan<sup>1d</sup>

Centre de Recherches sur les Macromolécules Végétales (CNRS), 53 X, 38041 Grenoble Cedex, France; Laboratoire de Minéralogie-Cristallographie (ERA 600), Université Claude Bernard, Lyon, France; and Département de Chimie, Université de Montréal, Montréal, Canada. Received August 5, 1977

**ABSTRACT:** The three-dimensional structure of cellulose triacetate II (CTA II) was derived from an x-ray and electron diffraction analysis using intensity data from fiber and single-crystal patterns. The unit cell is orthorombic with space group  $P_{2_1}2_{12_1}$  and dimensions  $a = 24.68 \text{ \AA}$ ,  $b = 11.52 \text{ \AA}$ , and  $c$  (fiber axis) =  $10.54 \text{ \AA}$ . A CTA II Model was built from the known structure of the central residue of cellotriose undecaacetate. This model was first refined through a conformational and packing analysis and then tested against the diffraction information. The resulting structure consists of antiparallel pairs of parallel CTA II chains. In projection, it has the same gross feature as the projection proposed earlier by Dulmage but it differs extensively in its details such as the glucose ring geometry and the conformation of the acetyl groups. Acetyl groups linked to C(6) are in the gg conformation. Those linked to C(2) and C(3) adopt the planar geometry identical to the one always found in the crystalline structure of acetyl sugars.

The well-known polymorphism in cellulose science and technology<sup>2a</sup> is found also in cellulose derivatives. Perhaps the most familiar case is the cellulose triacetate (CTA) system where the terminology CTA I and CTA II reflects the following reversible and nonreversible crystalline transformations (scheme A). Scheme A of transformation was clearly established by Sprague et al. in 1958<sup>2b</sup> and despite a few controversial reports<sup>3,4</sup> this scheme is now widely accepted.



Our recent morphological and structural study<sup>5-7</sup> of the polymorphic transformation of *valonia* cellulose followed

closely Sprague's scheme; at the supermolecular level, CTA I and CTA II were found to have specific morphologies closely related to those of cellulose I and cellulose II. This indicated that the polarity of the chains was preserved in going from cellulose I to CTA I or cellulose II to CTA II. Recent studies overwhelmingly support the antiparallel arrangement for cellulose II.<sup>8,9</sup>

A crystallographic study of CTA II was performed in 1957 by Dulmage.<sup>10</sup> His data suggested that the most probable space group was  $P_{2_1}$  with two pairs of parallel cellobiose acetate units per monoclinic unit cell. The corner pair and center pair were antiparallel and the overall arrangement was extremely close to that corresponding to the space group  $P_{2_12_12_1}$ .

Since this work on the two-dimensional arrangement of the chains was published, no further attempt had been made to date to obtain the complete structure in three dimensions. Knowledge on the structural aspects of carbohydrate moieties,<sup>11</sup> the effect of acetate substitution,<sup>12</sup> etc., has accumulated since then. The availability of the crystal structure data on  $\beta$ -cellobiose acetate<sup>13</sup> and  $\beta$ -cellotriose acetate<sup>14</sup> is a great advantage in an attempt to solve the CTA structure. A combined approach, involving conformational analysis of the chain, packing of the chain in the lattice, and the x-ray or electron diffraction data has been very successful in the analysis of complex polysaccharide structures.<sup>15,16</sup>

Finally, a new step in polymer crystalline structure analysis consists of the use of single-crystal  $hk0$  electron diffraction data from polymer single crystals. Such data are of great value to establish the symmetry elements of the base plane of the crystal. They also provide a wide range of  $hk0$  diffraction intensities, far in excess of the corresponding  $hk0$  from x-ray patterns. It was shown recently<sup>17</sup> that the electron-diffraction intensities on thin organic polymer crystals followed the kinematical approximation. These intensities can consequently be used to determine the structure of the base plane projection of polymer crystals.<sup>18,19</sup> For CTA II, single-crystal electron-diffraction diagrams containing over 40 independent reflections can be obtained.<sup>20</sup> These diagrams are indicative of a  $P_{2_12_12_1}$  symmetry for CTA II instead of  $P_{2_1}$  as proposed by Dulmage.<sup>10</sup> With all these new data and methods the CTA II structure has been reexamined. The aim was to achieve the most reliable three-dimensional solution based on the best possible experimental data: x-ray and electron-diffraction data on the polymer, crystal structure of the oligomers and conformational and packing analysis of the polymer.

## Experimental Section

CTA fibers suitable for x-ray diffraction were spun from methylene chloride-methanol solution.<sup>45</sup> Bundles of fibers were stretched (120%) at 200 °C for 15 min. Crystallinity was further improved by annealing in a water-vapor atmosphere at 190 °C for a few minutes in an autoclave.

The preparation of CTA single crystals and the observation of the electron-diffraction diagram were described previously.<sup>20</sup> Diagrams used for reliability factor calculation contained 22 independent diffraction spots and no double diffraction effects. Those used for Fourier synthesis had around 50 independent diffraction spots and contained some double-diffraction effect which was evaluated.

Fibers used for electron diffraction were prepared from *valonia* cellulose.<sup>5</sup>

X-ray diffraction experiments were performed on a Siemens Kristalloflex-2 diffraction unit equipped with a Warhus flat or cylindrical film camera. Kodak Kodirex films were used. The electron and x-ray intensities were measured by integration with a Joyce-Loebl Mark III recording densitometer. Whereas electron diffraction intensities were used directly, x-ray ones were corrected in the usual way for multiplicity, Lorentz and polarization factors,<sup>21</sup> reflection arcing, film-scanning direction (other than radial), and Cox and Shaw coefficient.<sup>22</sup> Unobserved x-ray reflections were estimated to be half of the threshold value. As usual, meridional reflections were discarded and due to the poor resolution of the upper layer lines of the x-ray

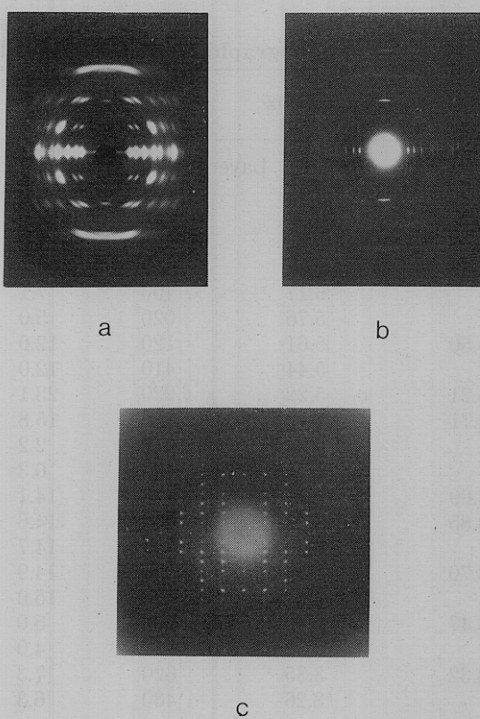


**Figure 1.** Diffraction diagrams used for the determination of the CTA II structure: (a) x-ray fiber diagram; (b) electron-diffraction fiber diagram; (c) single-crystal electron-diffraction diagram.

pattern, only the layers 0, 1, and 2 were considered. The individual intensities of overlapping equatorial reflections were resolved by comparison with the single-crystal electron-diffraction intensities after scaling both sets of intensities.

## Results and Discussion

**1. Strategy.** Generally, in order to resolve a polymer structure such as a polysaccharide, two kinds of data are used: the experimental x-ray fiber-diffraction diagram and the standard values for the bond lengths and angles of the repeat unit. As stated in the introductory section, our approach is supplemented by further experimental information coming from the study of CTA II single crystals and the crystallography of the corresponding oligomers. The general resolution procedure can be outlined as follows.

At first, the unit cell and the space group are deduced from x-ray and electron-diffraction analysis. A CTA chain is then built from the crystallographic coordinates of cellotriose undecaacetate and its energy is minimized through a conformational analysis where the sugar units are rotated about the glycosidic linkages and the acetyl groups about their linkages. Because of the mobility of the acetyl groups, especially those linked to the C(6) carbon atom, no absolute energy minimum can be determined but rather a zone of acceptable energy. Staying in such a zone, all the conformations are tested against the experimental x-ray and electron-diffraction data. In each case the reliability factor is computed and the packing energy of the crystal determined. From among all the possible structures having a satisfactory reliability factor, the final choice is based on packing considerations. Finally, the positions of the acetals at C(6) are ascertained through a Fourier synthesis using electron-diffraction intensity data.

**2. Unit Cell and Space Group Determination.** In Dulmage's study<sup>10</sup> a  $P_{2_1}$  space group and a monoclinic angle of 90° were proposed for CTA II. A careful reexamination of the x-ray and electron-diffraction diagrams indicated clearly that the structure possesses higher symmetry and that all reflections can be indexed according to the higher symmetry of the  $P_{2_12_12_1}$  space group. The diffraction data supporting this conclusion are shown in Figure 1 which represents the x-ray

**Table I**  
**Crystallographic Data for CTA II Deduced from X-Ray Fiber Diagrams (Final Model)**

d spacing (obsd)	d spacing (calcd)	Index	$F_o$	$F_c$	d spacing (obsd)	d spacing (calcd)	Index	$F_o$	$F_c$
Layer Line 0									
10.43	12.34	200	2.5	3.3	3.57	3.53	131		
8.40	10.44	110	18.7	18.6	3.52	3.46	521	7.4	5.6
6.67	8.42	210	24.5	24.5	3.31	3.34	231		
	6.69	310	24.5	29.2		3.30	701	8.4	5.1
	6.17	400	7.1	14.9		3.21	331		
	5.76	020	5.0	8.6		3.19	711		
5.50	5.61	120	12.0	17.0	3.15	3.11	621	6.5	10.7
	5.44	410	12.0	20.4		2.96	431		
5.21	5.22	220	23.1	35.1		2.91	801		
4.71	4.72	320	15.8	16.0	2.90	2.89	531	12.0	12.0
	4.54	510	2.2	0.7		2.87	721		
	4.21	420	6.3	5.0		2.87	811		
4.09	4.11	600	14.1	10.0					
3.85	3.87	610	14.6	3.2	5.26	5.27	002		
	3.79	130	14.7	16.5	5.30	5.15	102	3.2	5.1
3.70	3.75	520	14.9	14.9		4.85	202	2.0	0.5
	3.67	230	15.0	14.8	4.79	4.79	012	13.4	7.7
3.47	3.48	330	5.0	4.2		4.70	112		
	3.37	710	4.0	2.6		4.47	212	14.9	11.2
3.32	3.35	620	7.3	4.4	4.45	4.44	302		
	3.26	430	6.3	7.2	4.16	4.14	312	3.7	7.8
Layer Line 1									
9.67	9.69	101	5.0	4.6	3.88	4.01	402	2.0	3.0
7.96	8.01	201	2.5	3.9		3.89	022	9.2	8.2
	7.78	011	9.4	8.5	3.74	3.84	122		
7.39	7.42	111				3.78	412	10.0	10.5
6.53	6.58	211	11.1	9.6		3.71	222		
	6.49	301				3.60	502	3.7	7.2
5.66	5.65	311	4.7	10.8	3.45	3.52	322	3.7	3.1
	5.32	401			3.29	3.44	512	13.8	11.5
5.04	5.05	021	27.3	14.8		3.24	422	9.9	9.8
	4.95	121				3.12	602		
4.84	4.83	411	23.3	15.5		3.10	612		
	4.68	221			3.07	3.08	032		
4.15	4.47	501	4.0	8.0		3.05	132	19.3	16.5
	4.31	321	16.7	10.0		3.01	522		
3.89	4.17	511			2.90	2.93	232		
	3.91	421	7.6	5.2		2.90	702	5.5	10.0
	3.83	601	2.0	1.6		2.84	332		
	3.64	611			2.80	2.83	712		
3.62	3.61	031	8.8	7.8		2.77	622	7.8	8.1
						2.77	432		

diffraction fiber diagram (Figure 1a), the electron diffraction fiber diagram (Figure 1b), and the electron diffraction of a single crystal (Figure 1c). The electron fiber diagram (Figure 1b) confirms the absence of odd order 001 reflections and supports the  $2_1$  symmetry along the  $c$  axis. This is less clear in the x-ray fiber diagram shown in Figure 1a and the absence of an odd order reflection, such as 003, can be stated conclusively only after proper tilting of the specimen in the x-ray camera.<sup>23</sup> The symmetry in the  $ab$  plane is best deduced from the single-crystal electron-diffraction diagram (Figure 1c) which displays around 50 independent reflections in one quadrant symmetrically repeated in the three others. Moreover, along both  $a^*$  and  $b^*$ , all odd order  $h00$  and  $0k0$  reflections are absent whereas some of the even are present. These findings ascertain the presence of two orthogonal  $2_1$  axes along  $a$  and  $b$ . Consequently, the  $P_{2_12_12_1}$  space group was chosen for CTA II.

Tables I and II present a list of spacings and structure factors measured in the x-ray fiber diagram and the single-crystal electron-diffraction diagram. Following these measurements, a refinement of the unit cell gives:  $a = 24.68 \text{ \AA}$ ,  $b = 11.52 \text{ \AA}$ , and  $c$  (chain axis) =  $10.54 \text{ \AA}$ . These parameters which differ only slightly from Dulmage's data<sup>10</sup> give a set of calculated spacings which match closely the observed  $d$  spacings as seen

in Table I. From the volume of the unit cell and the density of  $1.29 \text{ g/cm}^3$ , eight acetyl glucose residues must be present in the unit cell. These residues are related through the symmetry of the space group which gives four equivalent positions in the unit cell. The choice is thus: either four chains with two acetyl glucose per repeat unit or two chains with four acetyl glucose per repeat unit. No valid argument supported this latter possibility and following Dulmage an arrangement with four acetyl cellobiose residues was selected.

**3. Definition of the Chain.** In the study with the oligomers of cellulose triacetate,<sup>13,14</sup> it was found that important crystallographic information on the polymer could be deduced from the study of the trimer, cellobiose undecaacetate.

In this molecule, the middle and nonreducing residues are approximately related through a  $2_1$  symmetry element with a translation axis of  $5.28 \text{ \AA}$  parallel to the chain axis. Within experimental error, this distance is exactly the "repeat distance" for the polymer. Thus the central triacetyl glucose residue of cellobiose undecaacetate appears to be a good starting unit to generate a model of CTA II chain with a two-fold screw axis, the location of this screw axis with respect to the chain being the same as in the trimer. This starting model has two advantages: all residues are geometrically equivalent and are linked in a regular conformation; it fits closely the

**Table II**  
Crystallographic Data for CTA II Deduced from Single-Crystal Electron-Diffraction Diagram (Final Model)

$h k 0$	$F_o$	$F_c$	$h k 0$	$F_o$	$F_c$
200	3.8	2.4	120	11.0	17.5
400	9.5	11.0	220	18.2	31.6
600	14.1	11.6	320	17.3	16.5
110	18.7	14.7	420	5.5	3.1
210	22.4	20.2	520	14.5	14.2
310	21.9	23.4	620	8.9	6.2
410	11.0	13.2	720	7.1	7.1
510	3.9	4.4	130	17.3	18.5
610	18.7	3.9	230	16.7	19.1
710	4.5	5.2	330	5.0	4.3
020	5.5	7.9	430	6.3	9.4

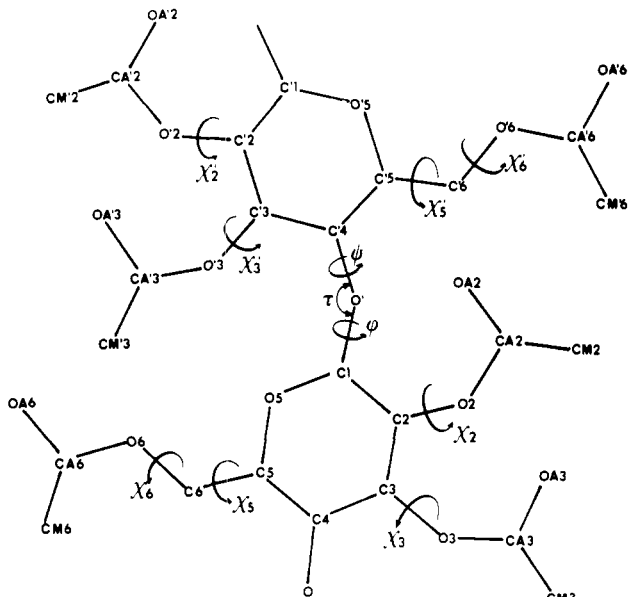


**Figure 2.** Atom numbering in acetyl cellobiose repeating unit and identification of the conformation angles used throughout the refinement.

actual crystalline geometry of the oligomers from which it is derived. Our approach differs from that of Zugenmaier and Sarko<sup>24</sup> who used standard carbohydrate bond lengths and angles to initiate the chain. In their approach, these values are modified throughout the energy refinement. In the present case, the selected bond length and angle values for the glucose residue are identical to those of the central residue of the trimer. These values are kept constant throughout the refinement which affects only the conformation angles  $\varphi$ ,  $\psi$ , and  $\tau$  and the torsion angles of the acetyl groups (Figure 2).

**4. Conformational Analysis of the Isolated Chain.** This analysis was performed using the virtual bond method which is particularly suitable to generate a polysaccharide chain of known repeat distance and helicity.<sup>25</sup> In this method, all the possible conformations are generated by rotation of the residues around the virtual bond. If  $\theta$  is the angle of this rotation, one specific conformation is then simply defined by a given  $\theta$  which can be related to the polysaccharide conformational angles  $\varphi$ ,  $\psi$ , and  $\tau$ . Figure 3 shows the correlations existing between  $\theta$ ,  $\varphi$ ,  $\psi$ , and  $\tau$  for a theoretical chain of cellulose triacetate built as described above and constrained within the unit cell. If  $\tau$  is to be kept below a maximum value of  $120^\circ$ ,<sup>26</sup> part of the  $\tau$  curve in full line,  $\varphi$  and  $\psi$  have the possibility of varying from  $-10^\circ$  to  $+19^\circ$  and from  $-25^\circ$  to  $+15^\circ$ , respectively.

For each value of  $\theta$ , an evaluation of the conformational energy of the chain was made. This energy is a sum of the nonbonded and electrostatic interactions between atoms of

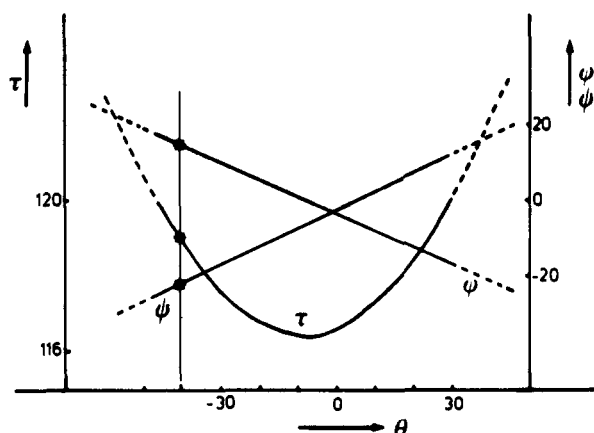


**Figure 3.** Correspondence between  $\theta$ ,  $\tau$ ,  $\varphi$ , and  $\psi$ . The vertical line indicates the final values of the model. The origin of  $\theta$  is arbitrary.  $\varphi$  is zero when H(1), C(1), O', C(4) is cis. It is positive when rotation is clockwise when looking from C(1), O'.  $\psi$  is zero when C(1), O', C'(4), H'(4) is cis. It is positive when rotation is clockwise when looking from O', C(4).

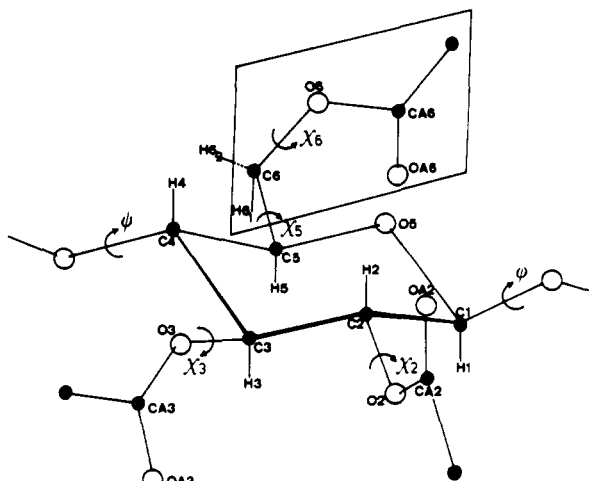


**Figure 4.** Definition of the conformation angles of the acetyl groups.  $\chi(2) = 0$  when H(2) and CA(2) are eclipsed and also when C(2) and OA(2) are eclipsed. For  $\chi(3)$ , the definition is similar with H(3) and CA(3) and C(3) and OA(3).  $\chi(5) = 0$  when H(61) and H(5) are eclipsed.  $\chi(6) = 0$  when H(61) and CA(6) are eclipsed and also C(6) and OA(6).  $\chi(2)$  is positive when rotation is clockwise when looking from C(2), O(2). Similar definition for  $\chi(3)$  and  $\chi(6)$ .  $\chi(5)$  is positive when rotation is clockwise when looking from C(5), C(6).

two contiguous residues. In the present study, the additional minor contribution to the energy due to the bond angle strain when  $\tau$  is varied was not included. Both the nonbonded and electrostatic interactions were calculated according to the procedure and parameters defined by Marchessault and Sundararajan.<sup>12</sup> For the electrostatic energy evaluation, a set of atomic partial charges slightly different from those defined in ref 12 was computed using the PCILo method.<sup>27–30,46</sup> The values of these charges for each atom of a residue as defined in Figures 2 and 4 are given in Table III.

When  $\theta$  was varied, no acceptable energy minimum was observed despite a noticeable improvement when  $\varphi$  went from the negative values toward positive area. The lack of a suitable minimum resulted from close contacts between the atoms belonging to the acetyl group linked to C(6) and the rest of the molecule. Initially, this group as well as the acetyl groups at C(2) and C(3) were kept fixed as in the central residue of cellobiose undecaacetate while  $\theta$  was varied. The rotation of the acetyl groups themselves has thus to be considered in order to minimize the conformational energy. Such an approach was already followed by Panov and Zhbankov<sup>31</sup> in their confor-

**Table III**  
**Partial Charges (as Fraction of the Electronic Charge)**  
**Assigned for the Atoms in Glucose Triacetate**

Atoms	$q_i$	Atoms	$q_i$	Atoms	$q_i$
O(4)	-0.215	O(3)	-0.217	OA(5)	-0.261
C(4)	0.125	CA(3)	0.33	CM(5)	0
C(1)	0.247	OA(3)	-0.261	H(61)	0
C(2)	0.101	CM(3)	0	H(62)	0
O(2)	-0.211	C(5)	0.089	H(1)	-0.025
CA(2)	0.330	O(5)	-0.211	H(2)	0.001
OA(2)	-0.261	C(6)	0.131	H(3)	0.01
CM(2)	0	O(6)	-0.20	H(4)	0
C(3)	0.127	CA(5)	0.33	H(5)	0.007

mational analysis of cellulose triacetate. Our starting hypothesis however differed from theirs since they excluded the possibility of  $2_1$  symmetry along the polymer chain. Since this is our working hypothesis confirmed by the data on oligomers crystallography, their results cannot be applied here.

The variations of the acetyl torsion angles  $\chi(2)$ ,  $\chi(3)$ ,  $\chi(5)$ , and  $\chi(6)$  as defined in Figure 4 were then considered in the next step of the refinement. This implied the addition of new torsional energy terms to the sum of nonbonded and electrostatic interaction energies already considered. Torsional energies defined by a function of the form  $U = U_0(1 + \cos 3\chi)$  were calculated<sup>32</sup> for  $\chi(2)$ ,  $\chi(3)$ ,  $\chi(5)$ , and  $\chi(6)$ . A value of 1.5 kcal/mol was assigned to  $U_0$  for  $\chi(2)$ ,  $\chi(3)$ , and  $\chi(6)$  whereas 3.0 kcal/mol was used in the case of  $\chi(5)$  which involved the rotation of a larger number of atoms. The refinement was achieved through an iterative procedure,<sup>33</sup> using a chain of four residues linked by conformational angles close to those observed in the central residue of the trimer, i.e.,  $\tau = 118.9^\circ$ ,  $\varphi = 15.0^\circ$ , and  $\psi = -21.9^\circ$ . In each of the four residues, the four torsion angles of the acetyl groups were varied independently and the energy of the central disaccharide was evaluated. A suitable energy minimum was found which corresponded to identical values for the torsion angles of the acetyl groups in each of the residues of the disaccharide considered. The values obtained were  $\chi(2) = +20^\circ$ ,  $\chi(3) = -15^\circ$ ,  $\chi(5) = -60^\circ$  ( $O(6)$  in the gg<sup>47</sup> position) and  $\chi(6) = +25^\circ$ . The first three values are equivalent to the starting model whereas  $\chi(6)$  varied markedly from its starting value of  $+60^\circ$ .

It is known that acetyl groups linked to the C(6) position are rather mobile. This means that the minimum energy found must be surrounded with a more or less large area of almost equivalent favorable energy when  $\chi(5)$  and  $\chi(6)$  are varied.

The energy of the central disaccharide described as above was then computed for each  $\chi(5)$  and  $\chi(6)$  rotation. In each of the residues  $\chi(5)$  and  $\chi(6)$  were kept the same (i.e., related by  $2_1$  symmetry) and for each set of  $\chi(5)$ ,  $\chi(6)$  values,  $\chi(2)$  and  $\chi(3)$  were adjusted to give the energy minimum. An energy contour map as a function of  $\chi(5)$  and  $\chi(6)$  was then obtained. Most of the values of  $\chi(5)$  and  $\chi(6)$  lead to energetically forbidden conformations. It is only in the area shown in Figure 5 that a suitable minimum area could be obtained. The main feature of this map is the shape of the minimum which occurs as a narrow elongated area where  $\chi(5) = -60^\circ$  (gg position for  $O(6)$ ) while  $\chi(6)$  varies from  $A = +25^\circ$ , the absolute minimum, to  $B = -30^\circ$ , a secondary minimum of almost the same energy. A map such as shown in Figure 5 demonstrates the flexibility of  $\chi(6)$  which can change by  $55^\circ$  without affecting the conformational energy drastically. If  $\chi(6)$  takes the value of  $+60^\circ$  as in the central residue of the trimer, an unacceptable energy value results.

In the next step of the refinement, the conformation of the chain was slightly altered by changing  $\theta$ . Maps similar to the one shown in Figure 5 were obtained with minimum energies located at about the same values for  $\chi(5)$  and  $\chi(6)$ .

The foregoing energy calculations allow definition of an



**Figure 5.** Conformational energy of a hexacetyl cellobiose residue (kcal/mol) taken from a CTA II chain having  $2_1$  symmetry, as a function of  $\chi(5)$  and  $\chi(6)$ . Points A and B indicate the two energy minima. The adjacent stars correspond to position obtained after the refinement for the C(6) acetyl group exterior and interior to the pair of chains.

"average" minimum energy chain which can be now tested in a packing study and evaluated against observed x-ray intensities. The chain consists of glucose residues having bond lengths and angles as in the central residue of cellotriose undecaacetate. These residues are connected with the conformational angles  $\tau = 118.9^\circ$ ,  $\varphi = 15.0^\circ$ ,  $\psi = -21.9^\circ$ . The acetyl groups are defined by  $\chi(2) = +20^\circ$ ,  $\chi(3) = -15^\circ$ ,  $\chi(5) = -60^\circ$ , and  $\chi(6) = +25^\circ$ . In further refinements,  $\tau$  will be allowed to vary from  $117$  to  $120^\circ$ ,  $\chi(2)$  and  $\chi(3)$  from  $-25^\circ$  to  $+25^\circ$ ,  $\chi(5)$  from  $-85^\circ$  to  $-45^\circ$ , and  $\chi(6)$  from  $-50^\circ$  to  $+40^\circ$ .  $\chi$  values taken out of these ranges would lead to intrachain close contacts.

**5. Chain Packing Analysis.** The four chains of cellulose triacetate can be arranged in two ways inside the unit cell. In the first case, the chain can be disposed on the  $2_1$  axis parallel to the  $c$  direction, giving two sets of independent chains per cell. This type of packing involves ribbons of chains with parallel axes. This would certainly give a crystalline morphology different from the lozenges observed for the single crystals. Moreover, in the course of the refinement, it was found that such an arrangement gave poor agreement between calculated and observed x-ray intensities. Consequently this type of packing was rejected and the  $2_1$  unit cell axes were placed between the chains as proposed by Dulmage.<sup>10</sup> The polymer chains are thus related in pairs and there are two antiparallel pairs of chains per unit cell. Such unusual packing was never proposed before for other polysaccharide crystals but was already encountered at least in one case in the field of synthetic polymers, for poly(pentamethylene sulfide).<sup>35</sup>

When projected on the  $ab$  plane, two parameters are sufficient to define the projection of a pair of chains as shown in Figure 6a. The minimum energy chain defined above is initially disposed on a  $2_1$  axis of the unit cell parallel to  $c$ . It is then rotated through an angle  $\alpha$  and translated through a

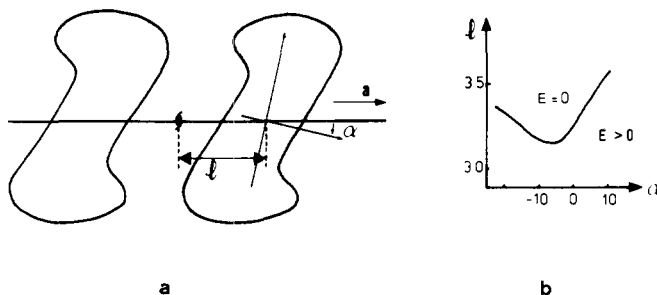


**Figure 6.** (a) Definition of the parameters used for the packing of a pair of CTA II chains viewed in projection on the  $ab$  plane. (b) Energy of packing as a function of the two parameters  $\alpha$  and  $l$ .

distance  $l$  along  $a$ . The second chain is then generated through the  $2_1$  symmetry. The packing energy of the pair was calculated by summing all the nonbonded energy interactions between the atoms of the two chains. Because of the large number of pairs of atoms, only the repulsion energies were included for and simple functions were used as follows:<sup>12,36,37</sup>

$$\begin{aligned} E_{ij} &= 0 && \text{for } d_{ij} \geq d_{ij}^0 \\ E_{ij} &= w_{ij}(d_{ij} - d_{ij}^0)^2 && \text{for } d_{ij} < d_{ij}^0 \end{aligned}$$

where  $d_{ij}$  is the distance between atoms  $i$  and  $j$ ,  $d_{ij}^0$  is an empirical cutoff distance, and  $w_{ij}$  is a weight for a given type of interaction.

The packing energy of the pair of chains as a function of the packing parameters  $\alpha$  and  $l$  is shown in Figure 6b. The curve delineates a zone of positive energy (below) and a zone of zero energy (above) for which all atom pair distances are greater than the cutoff distances. The packing situations corresponding to points on the curve or immediately below indicate the closest possible packing.

The packing of the pairs of chains in the unit cell necessitates the introduction of two new parameters which are defined in Figure 7. Here  $\beta$  is the rotation of the whole pair around its  $2_1$  symmetry axis whereas  $t$  corresponds to the translation along the unit cell parameter  $c$ , indicating the relative shift of two antiparallel pairs of chains. Interpair energy is then calculated as for the intrapair energy. For each acceptable  $\alpha$  and  $l$  value, sets of  $\beta$  and  $t$  which give a packing energy of reasonable value are determined. A complete exploration of the energy map when these parameters are varied shows that a suitable minimum energy can be found exclusively for values of  $l$  between 3.40 and 3.75 Å,  $\alpha$  between 0 and 10°,  $\beta$  between 17 and 25°, and  $t = -0.2c$ .

The best packing situation is shown in projection in Figure 7 where the various angles and translations have their optimum values. When the CTA II chain is slightly modified in further refinement, only minor adjustments are applied to the packing parameters which will remain essentially as in Figure 7.

**6. Structure Refinement from X-Ray and Electron-Diffraction Data.** Throughout the structure refinement from diffraction data, the classical reliability factor

$$R = \sum |F_o - F_c| / \sum F_o$$

was minimized, where  $F_o$  and  $F_c$  correspond to observed and calculated structure amplitudes.

The problem of overlapping intensities in the x-ray fiber diagram was solved differently for equatorial and nonequatorial reflections. For nonequatorial data, when two or more reflections were superimposed the corresponding calculated structure factor was evaluated as follows:

$$F_c = \left[ \sum_i (F_c^i)^2 \right]^{1/2}$$

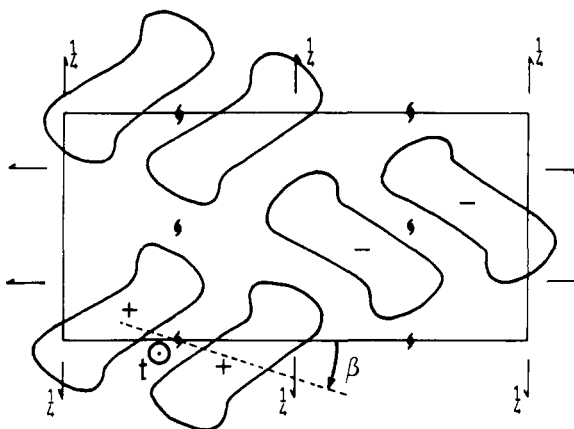


**Figure 7.** Packing of the pair of CTA II chains inside the unit cell. Definition of parameters  $\beta$  and  $t$ . The figure corresponds to the projection of the final packing.

Since x-ray and electron intensities for equatorial reflections are closely matched, overlapping x-ray intensities were decomposed according to electron intensities. This approach seems to be more accurate than the curve decomposition treatment used by Hindle and Johnson.<sup>38</sup> In their study of CTA II, the decomposition of the overlap of (320) and (220) reflections led to the intensity of (320) twice as strong as that of (220). The electron-diffraction data in Table II show that (320) has lower intensity than (220).

In order to define an electron-diffraction  $R$  factor, structure factors were also calculated from electron-diffraction intensities. The treatment of Vainshtein was applied<sup>39</sup> assuming quasi-kinematical scattering, as recently justified by Dorset<sup>17</sup> for thin organic crystals. Atomic scattering factors used throughout the calculation were those defined by Doyle and Turner.<sup>40</sup> An isotropic temperature factor of zero was chosen for the electron-diffraction intensities and a value of 10 for x-ray intensities.

The refinement consisted in minimizing the  $R$  factor as a function of the conformation and packing variables. Due to the large number of variables involved, the SIMPLEX method<sup>41</sup> was adapted for the refinement. As usually found with this type of program, false minima are often encountered. For this reason, sets of value for the structure variables were input in the refinement program which had to converge toward the same minimum. A minimum which was not obtained persistently was discarded.

With the electron-structure factor, the refinement concerned only the  $ab$  projection of the structure. The refinement converged toward the same molecular structure whether the hydrogen atoms were present or not. In order to limit the computing time, they were consequently omitted in subsequent calculations. A first approach to this refinement involved six independent conformation and packing variables defined above:  $\theta$ ,  $l$ ,  $\alpha$ ,  $\beta$ ,  $\chi(5)$ , and  $\chi(6)$ . For x-ray diffraction data which involved the three-dimensional structure,  $t$  was added as a seventh variable in the SIMPLEX procedure.

It was found that the parameters having the most effect on  $R$  were the angles  $\chi(5)$  and  $\chi(6)$  which define the position of the acetyl groups linked to C(6). These angles when varied control 25% of the total scattering material and their proper position is critical in order to obtain a suitable  $R$ . Moreover as seen above (Figure 5) two sets of acetyl torsional angles gave suitable minimization of the conformational energy of these acetyl groups. For this reason, it was decided also to study the case where one acetyl residue would have its C(6) acetyl group in the neighborhood of position A whereas the next residue on the chain would have its C(6) acetyl group close to position B. This slackens the  $2_1$  symmetry of the chain only for these

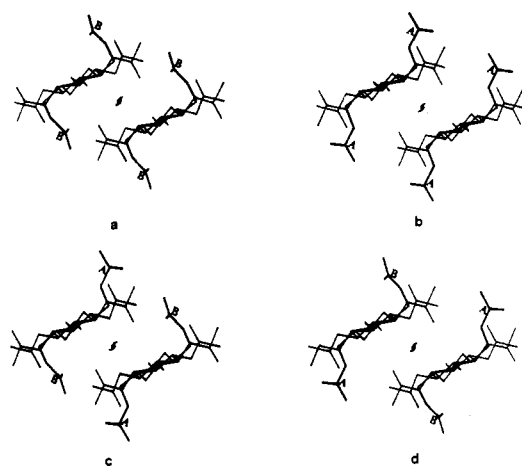


**Figure 8.** Different possibilities for the packing of the pair of CTA II chains, according to the conformations of the C(6) acetate: (a and b) the chain has  $2_1$  symmetry along its backbone; (c and d) the interior and the exterior C(6) acetyl groups are in different conformation. A and B refer to conformations defined in Figure 5.

groups and introduces two more variables  $\chi'(5)$  and  $\chi'(6)$  as defined in Figure 2. The rest of the chain however was kept under rigorous  $2_1$  symmetry even though this is not required by the crystallography since the chains are not positioned on privileged axes of the crystal. The  $2_1$  symmetry along the chain has several advantages: it gives the most regular shape to the chain and also leads to an easier packing of the CTA chains into pairs as shown in Figure 6. Furthermore, such a symmetry for the chain was already suggested in the crystal structure of cellobiose undecaacetate.<sup>14</sup>

Four cases are considered to initiate the refinement corresponding to the two positions available to the C(6) acetyl groups in the primed and unprimed residue. These starting positions are shown in Figures 8a and 8b which correspond to symmetrical positions of the acetate: the CTA II chain is assigned the  $2_1$  symmetry, and both acetates are either in conformation A or conformation B. On the contrary, in Figures 8c and 8d, the primed and unprimed residues have different conformations for the acetate linked to C(6).

Upon refinement, situations such as shown in Figures 8b and 8d did not yield an  $R$  factor below 0.38. On the contrary, cases such as shown in Figures 8a and 8c could refine to  $R$  values close to 0.30 with x-ray data and 0.26 with electron-diffraction data. In both Figures 8a and 8c, the C(6) acetate group interior to the pair of chains is in the conformation B. The two figures differ in the exterior C(6) acetate which is in the conformation B in Figure 8a and conformation A in Figure 8c.

**7. Fourier Refinement of the Acetate Group Linked to C(6).** A choice between the arrangements of Figures 8a and 8c was attempted through a Fourier refinement. This type of refinement, adapted from the NRC program of Ahmed,<sup>42</sup> uses the observed structure factor amplitudes obtained from the single-crystal electron-diffraction diagram and part of the molecule common to Figures 8a, 8b, 8c, and 8d. In the present case, the refinement involved, without restriction, the 45  $F_0$  corresponding to all the  $kh0$  reflexions with  $d$  spacings greater than 2 Å. Due to the small number of reflections considered, the precise location of the projection of the 72 atoms of the acetyl cellobiose was not expected but rather an overall shape of the projection of the molecule at 2 Å resolution. In principle, this should be enough to establish the positions of the C(6) acetates.

An electron potential map was thus created in Figure 9b from the part of the molecule shown in Figure 9a, where both acetyl groups were removed (removal of CA(6), OA(6), CM(6),

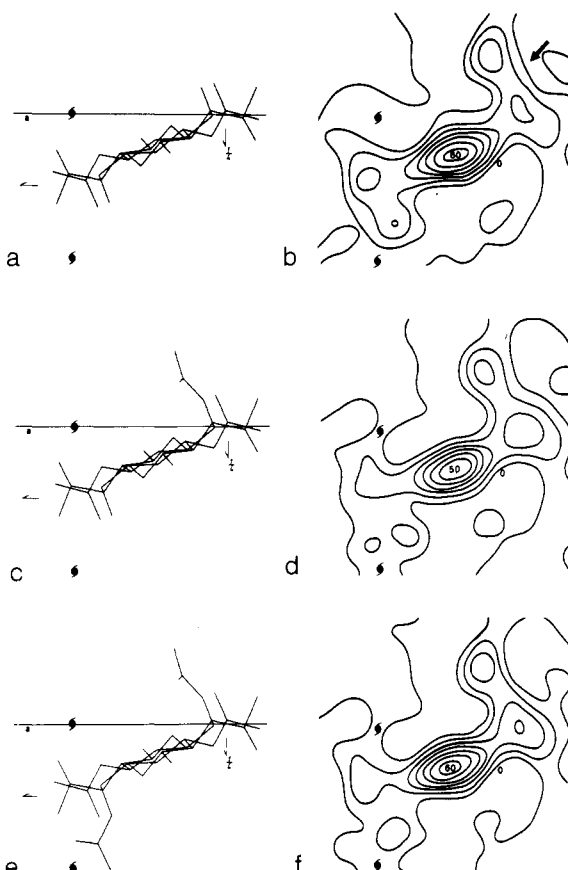


**Figure 9.** Electrostatic potential map obtained through a Fourier synthesis using electron-diffraction data of a single-crystal pattern. 9b corresponds to the part of the molecule shown in 9a (arrow points toward the interior C(6) acetyl group which is clearly revealed). 9d is obtained from 9c and 9f from 9e.

CA'(6), OA'(6), CM'(6)). In Figure 9b a zone of positive potential occurs (arrow) which clearly outlines the position of the C(6) acetate interior to the pair of chains. This acetyl group has the conformation B as deduced above when minimizing the  $R$  factor in the x-ray and electron-data refinement. Since the other acetyl group was not as well resolved, a further electron potential map was generated using a larger number of atoms of the CTA II molecule.

This second map is shown in Figure 9d. It derives from the part of the molecule drawn in Figure 9c, where only the interior C(6) acetate is well positioned. Here again, it is not possible to locate the exterior C(6) acetate with certitude. This uncertainty was not relieved even when fixed positions were given for this acetate group. This is illustrated in Figures 9e and 9f where the conformation A was imposed for the exterior C(6) acetate (Figure 9e). The resulting map (Figure 9f) did not confirm such hypothesis. Similar negative results were obtained when other conformations were also given to this acetate group. Further improvements in the refinement were also sought, using difference Fourier analysis. This method however was unsuccessful in bringing newer details in the calculated maps. The failure of the Fourier refinement to give clearly the shape of the CTA II molecule in the region of the C(6) acetate may be due to two reasons: (a) there are not enough diffraction data to give a significant Fourier refinement; (b) the C(6) acetyl group considered does not have a fixed conformation but assumes rather a statistical or disordered position in going from one acetyl cellobiose to the next (some of these groups are in conformation B and some in conformation A, or even intermediate conformations).

It may be recalled here that the single crystals and the an-

**Table IV**  
Fractional Atomic Coordinates for one Acetyl Cellobiose Residue (Final Model of CTA II)

Atom	x/a	y/b	z/c
O	0.362	-0.083	0.405
C(4)	0.385	-0.133	0.517
C(1)	0.393	-0.096	0.789
C(2)	0.445	-0.082	0.704
O(2)	0.475	0.012	0.758
CA(2)	0.529	-0.010	0.779
OA(2)	0.550	-0.093	0.747
CM(2)	0.550	0.098	0.848
C(3)	0.430	-0.051	0.570
O(3)	0.478	-0.078	0.496
CA(3)	0.500	0.015	0.434
OA(3)	0.480	0.109	0.426
CM(3)	0.556	-0.017	0.382
C(5)	0.337	-0.135	0.613
O(5)	0.360	-0.180	0.731
C(6)	0.293	-0.212	0.576
O(6)	0.312	-0.317	0.528
CA(6)	0.287	-0.416	0.571
OA(6)	0.250	-0.407	0.637
CM(6)	0.310	-0.516	0.507
O'	0.410	-0.134	0.905
C'(4)	0.386	-0.084	1.017
C'(1)	0.378	-0.121	1.289
C'(2)	0.327	-0.135	1.204
O'(2)	0.296	-0.229	1.258
CA'(2)	0.243	-0.206	1.279
OA'(2)	0.221	-0.124	1.247
CM'(2)	0.221	-0.315	1.348
C'(3)	0.342	-0.166	1.069
O'(3)	0.293	-0.139	0.995
CA'(3)	0.271	-0.232	0.934
OA'(3)	0.291	-0.326	0.926
CM'(3)	0.215	-0.199	0.882
C'(5)	0.434	-0.082	1.113
O'(5)	0.411	-0.036	1.231
C'(6)	0.479	-0.005	1.076
O'(6)	0.460	0.091	1.009
CA(6)	0.427	0.167	1.073
OA'(6)	0.420	0.152	1.179
CM'(6)	0.414	0.264	0.992

nealing of the fibers of CTA II were made at 250 °C. At such temperature, one may expect extensive mobility of a flexible group such as a C(6) acetate. This hypothesis is supported by the fact that intensities of some reflections such as for instance  $I_{600}$  and  $I_{610}$  could never be simultaneously adjusted with the same model. Their adjustment could only occur when a statistical distribution of the C(6) acetyl group was considered. Despite this finding and in order to limit the number of independent variables in the SIMPLEX refinement program, it was decided to avoid the statistical hypothesis in the present work.

The choice between the models shown in Figures 8a and 8c was made on the basis of packing energy considerations. Only in the model presented in Figure 8c could most of the poor contacts be avoided, especially by small rotations of the acetate groups linked to C(2) and C(3). After several cycles of refinement, the final model when tested against diffraction data yielded a reliability factor of 0.30 with x-ray data and 0.26 with electron-diffraction data. The list of the calculated structure factors  $F_c$  obtained with our final model is presented in Tables I and II for x-ray and electron data.

#### Description of the Structure

A list of the final atomic coordinates is presented in Table IV. These coordinates yield the three-dimensional picture of the chain shown in Figure 10. The final conformational and

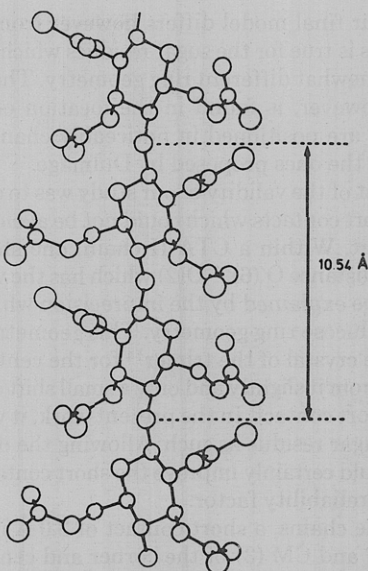


**Figure 10.** Perspective view along the fiber axis of a CTA II chain as drawn by the ORTEP program.<sup>44</sup>

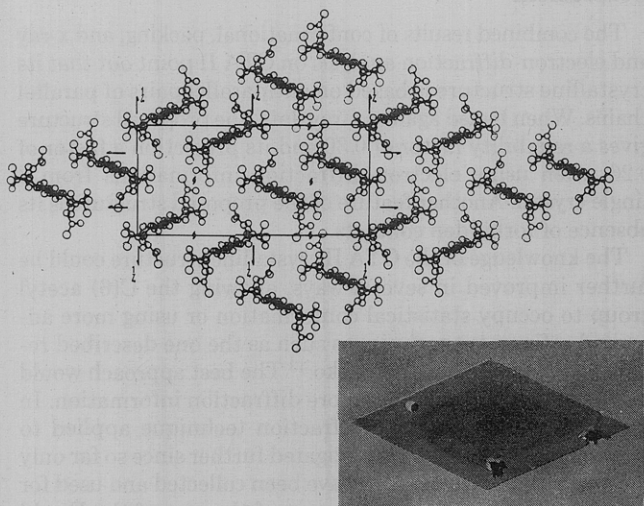


**Figure 11.** ab plane projection of the CTA II structure. Insert: Single crystal of CTA II properly oriented with respect to the projection.

packing parameters are:  $\alpha = 6.07 \text{ \AA}$ ,  $l = 3.58 \text{ \AA}$ ,  $\beta = 20.50^\circ$ ,  $t = 0.19^\circ\text{C}$ ;  $\varphi = 15.4^\circ$ ,  $\psi = 22.3^\circ$ ,  $\tau = 119.1^\circ$ ,  $\chi(2) = 6.5^\circ$ ,  $\chi(3) = 0.0^\circ$ ,  $\chi(5) = -73.7^\circ$  (gg conformation),  $\chi(6) = 24.4^\circ$ ,  $\chi'(5) = -83.4^\circ$  (gg conformation),  $\chi'(6) = -45.4^\circ$ .

The packing of the chains in the crystal is shown in projection in Figure 11 which shows also the electron micrograph of a single crystal properly oriented with respect to the molecule arrangement. In Figure 11, one sees that the (110) growth planes of the crystal are indeed parallel to the direction of the highest atomic densities, as expected. The occurrence of (210) and (310) as twinning planes<sup>20</sup> may also be explained since these directions intersect the structure without encountering too many atoms.

The projection such as the one shown in Figure 11 may be compared with the one presented earlier by Dulmage.<sup>10</sup> The gross features are the same; the structure consists of pairs of parallel CTA II chains connected through the 2<sub>1</sub> screw axis positioned outside of the chains. In the unit cell there are two pairs of chains, the pairs being antiparallel with respect to one another. This is consistent with the reversible solid state transformation CTA II  $\rightleftharpoons$  cellulose II, since in the cellulose II crystals there are also chains of different polarities.<sup>8,9</sup> At a

finer scale, our final model differs however from the one of Dulmage. This is true for the sugar residues which in our work displays a somewhat different ring geometry. The important difference, however, is found in the location of the acetyl groups which are positioned in noticeably changed conformations from the ones proposed by Dulmage.

Another test of the validity of our study was to evaluate the number of short contacts which could not be avoided through the refinement. Within a CTA II chain, one short contact occurs in the distance O'(6) ... O(2) which has the value of 2.83 Å. This may be explained by the imprecision which exists in defining the glucose ring geometry. This geometry is the one defined in the crystal of the trimer<sup>14</sup> for the central residue. It may differ from it slightly and only a small shift of the atoms will lift the short contact. In the present work, it was decided to keep the sugar residue as such. Allowing the deformation of the ring would certainly improve the short contact situation as well as the reliability factor.

Between the chains, a short contact of 3.0 Å is found between CM'(6) and CM'(3) of the corner and central chains. Such contact involves a C(6) acetyl group which may have a statistical position as seen above. This again was not considered to be a serious disadvantage of the proposed model.

## Conclusions

The combined results of conformational, packing, and x-ray and electron-diffraction analysis on CTA II point out that its crystalline structure is based on antiparallel pairs of parallel chains. When tested against x-ray data, the proposed structure gives a reliability factor of 0.30 and its projection a factor of 0.26 when using electron-diffraction informations from a single crystal. Another feature of the proposed structure is its absence of forbidden contacts.

The knowledge of the CTA II crystalline structure could be further improved in several ways, allowing the C(6) acetyl group to occupy statistical conformation or using more advanced refinement techniques such as the one described recently by Zugenmaier and Sarko.<sup>43</sup> The best approach would be however to try to obtain more diffraction information. In this respect, the electron-diffraction technique applied to single crystals should be investigated further since so far only the  $hk0$  reflexion intensities have been collected and used for the refinement. If the rest or part of the rest of the Ewald sphere could also be explored, up to several hundred diffraction informations could be used for the refinement.

**Acknowledgments.** This work was supported by the France-Québec Scientific exchange program. It was also funded through an ATP of the CNRS on tridimensional structure of biological molecules. The authors acknowledge the help of Professor Gagnaire for the use of his computing facilities. Special thanks are also due to Mr. Tran Vinh for calculating Table III and Mr. A. Thozet for helpful discussions and assistance in preparing the ORTEP plots.

## References and Notes

- (1) (a) Taken in part from a doctoral thesis presented by E. Roche to the Université de Grenoble; (b) Centre de Recherches sur les Macromolécules Végétales; (c) Université Claude Bernard; (d) Université de Montréal.
- (2) (a) N. M. Bikales and L. Segal, Ed., "Cellulose and Cellulose Derivatives", Part IV, Wiley-Interscience, New York, N.Y., 1971; (b) B. S. Sprague, J. L. Riley, and H. D. Noether, *Text. Res. J.*, **28**, 275 (1958).
- (3) J. J. Creely and C. M. Conrad, *Text. Res. J.*, **35**, 184 (1965).
- (4) S. Watanabe, M. Takai, and J. Hayashi, *J. Polym. Sci., Part C*, **23**, 825 (1968).
- (5) H. Chanzy and E. Roche, *J. Polym. Sci., Polym. Phys. Ed.*, **12**, 2583 (1974).
- (6) H. Chanzy and E. Roche, *J. Polym. Sci., Polym. Phys. Ed.*, **13**, 1859 (1975).
- (7) H. Chanzy and E. Roche, *J. Polym. Sci., Appl. Polym. Symp.*, **28**, 701 (1976).
- (8) A. Sarko and R. Muggli, *Macromolecules*, **7**, 486 (1974).
- (9) F. J. Kolpak and J. Blackwell, *Macromolecules*, **9**, 273 (1976).
- (10) W. J. Dulmage, *J. Polym. Sci.*, **26**, 277 (1957).
- (11) S. Arnott and W. E. Scott, *J. Chem. Soc., Perkin Trans. 2*, 324 (1972).
- (12) R. H. Marchessault and P. R. Sundararajan, *Pure Appl. Chem.*, **42**, 399 (1975).
- (13) F. Leung, H. Chanzy, S. Perez, and R. H. Marchessault, *Can. J. Chem.*, **54**, 1365 (1976).
- (14) S. Perez and F. Brisse, *Acta Crystallogr., Sect. A*, **33**, 2578 (1977).
- (15) D. A. Rees, "Organic Chemistry Series One", Vol. 7, G. O. Aspinall Ed., Butterworths, London, 1975, p 251.
- (16) D. A. Brant, *Q. Rev. Biophys.*, **9**, 527 (1976).
- (17) D. L. Dorset, *Acta Crystallogr., Sect. A*, **32**, 207 (1976).
- (18) W. Claffey, K. Gardner, J. Blackwell, J. Lando, and P. Geil, *Philos. Mag.*, **30**, 1223 (1974).
- (19) Y. Y. Tomashpol'skii and G. S. Markova, *Vysokomol. Soedin.*, **6**, 274 (1964).
- (20) H. Chanzy and E. Roche, *J. Polym. Sci., Polym. Phys. Ed.*, **12**, 1117 (1974).
- (21) M. Kakudo and N. Kasai, "X-Ray Diffraction by Polymers", Elsevier, Amsterdam, 1972, p 282.
- (22) E. G. Cox and W. F. B. Shaw, *Proc. R. Soc. London, Ser. A*, **127**, 71 (1930).
- (23) L. E. Alexander, "X-Ray Diffraction Methods in Polymer Science", Wiley-Interscience, New York, N.Y., 1969, p 193.
- (24) P. Zugenmaier and A. Sarko, *Biopolymers*, **12**, 435 (1973).
- (25) P. R. Sundararajan and R. H. Marchessault, *Can. J. Chem.*, **53**, 3563 (1975).
- (26) W. T. Winter and A. Sarko, *Biopolymers*, **13**, 1461 (1974).
- (27) S. Diner, J. P. Malrieu, and P. Claverie, *Theor. Chim. Acta*, **13**, 1 (1969).
- (28) J. P. Malrieu, P. Claverie, and S. Diner, *Theor. Chim. Acta*, **13**, 18 (1969).
- (29) S. Diner, J. P. Malrieu, F. Jordan, and M. Gilbert, *Theor. Chim. Acta*, **15**, 100 (1969).
- (30) F. Jordan, M. Gilbert, J. P. Malrieu, and U. Pincelli, *Theor. Chim. Acta*, **15**, 211 (1969).
- (31) V. P. Panov and R. G. Zhabkov, *Vysokomol. Soedin. Ser. A*, **16**, 4, 807 (1974).
- (32) A. J. Hopfinger, "Conformational Properties of Macromolecules", Academic Press, New York, N.Y., 1973, p 119.
- (33) P. R. Sundararajan and R. H. Marchessault, *Biopolymers*, **11**, 829 (1972).
- (34) A. Sarko and R. H. Marchessault, *J. Polym. Sci., Part C*, **28**, 317 (1969).
- (35) Y. Gotoh, H. Sakakihara, and H. Tadokoro, *Polym. J.*, **4**, 68 (1973).
- (36) D. E. Williams, *Acta Crystallogr., Sect. A*, **25**, 464 (1969).
- (37) P. Zugenmaier and A. Sarko, *Acta Crystallogr., Sect. B*, **28**, 3158 (1972).
- (38) A. M. Hindle and D. J. Johnson, *Polymer*, **13**, 27 (1972).
- (39) B. K. Vainshtein, "Electron Diffraction Structure Analysis", Pergamon Press, Oxford, 1964.
- (40) P. S. Doyle and P. S. Turner, *Acta Crystallogr., Sect. A*, **24**, 390 (1968).
- (41) J. A. Nelder and R. Mead, *Comput. J.*, **7**, 308 (1965).
- (42) F. R. Ahmed, S. R. Hall, M. F. Pippy, and C. P. Huber, NRC Crystallographic Programs for the IBM/360 System, Division of Pure Physics, National Research Council, Ottawa, Canada, 1966–1968.
- (43) P. Zugenmaier and A. Sarko, *Biopolymers*, **15**, 2121 (1976).
- (44) C. R. Johnson, ORTEP, Oak Ridge National Laboratory, Report ORNL-3794, 1965.
- (45) This preparation was kindly performed by Dr. Sacco from Rhône-Poulenc Textile, Lyon.
- (46) Values kindly computed for us by Mr. Tran Vinh from the Centre d'Etudes Nucléaires de Grenoble.
- (47) For the definition of gg see ref 34.